Water Quality Analysis and Modeling of the Al-Rawdhatain Field, Kuwait

[1]Jasem M. Al-Humoud and [2]Fawzia M. Al-Ruwaih
[1]Department of Civil Engineering, College of Engineering and Petroleum,
[2]Department of Earth and Environmental Sciences, Faculty of Sciences,
Kuwait University, Kuwait, Kuwait

Abstract: The Al-Rawdhatain field is the main freshwater well in Kuwait. The fresh groundwater is produced in the Dibdibba Formation that is the upper formation of the Kuwait group aquifer. The latest annual field production was ~6 Million Imperial Gallons (MIG). The quality of the fresh groundwater in the study area is analyzed to determine the prevailing geochemical processes in the aquifer, groundwater chemistry and genesis types. In addition, the groundwater quality and water level trends of the field during the period of 1985-2017 are investigated. The source rock is identified and the chemical equilibrium of the groundwater with respect to the minerals in the aquifer matrix is assessed. The collected groundwater data were compiled, analyzed, plotted and interpreted. The analyses show that the Al-Rawdhatain field contains fresh groundwater. The salinity of the groundwater ranged from 530-1800 mgL^{-1} in 1966 from 400-1500 mgL^{-1} in 1991 and from 950 to 3210 mgL^{-1} in 2015, indicating an increase in the salinity with time. The chemical properties of the groundwater in the study field are dominated by alkaline earths which exceed alkalis and strong acids that exceed weak acids. The main groundwater chemistry comprises Na_2SO_4, $NaHCO_3$, $Ca(HCO_3)_2$ and $CaSO_4$. Generally, the groundwater exhibits an over saturation with respect to calcite and dolomite and undersaturation with respect to anhydrite, gypsum and halite. The PCO_2 ranges from 1.86-3.11×10^{-3} atm, representing a deep closed environment system. The application of the mass balance technique indicates that the ion exchange, reverse ion exchange, dissolution of gypsum, calcite precipitation (dedolomitization) and carbonate weathering are the prevailing geochemical processes in the Al-Rawdhatain field.

Key words: Confined aquifer, Al-Rawdhatain field, water quality, mass balance, salinity, chemistry

INTRODUCTION

Location of the study area: Kuwait covers an area of 17,818 km^2 (6880 mi^2) at the North Western shore of the Arabian Gulf between 28°30'-30°30'N and 46°30'-48°30'E in latitude and longitude, respectively. The greatest distance from North to South and from East to West is 200 km (120 mi) and 170 km (110 mi), respectively. It is an arid region which is marked by very scarce rainfall, high temperature and evaporation rates and a lack of perennial surface waters.

The Al-Rawdhatain field is Northeast of Kuwait city in the West of Kuwait on the Al-Abdally highway and between 30°03'N-29°46'N and 47°29'E-47°30' E (Fig. 1). The construction of water wells in the Al-Rawdhatain field started in September, 1962 and was completed in 1964 with the aim of producing 4 Million Imperial Gallons (MIG). However, the actual field production took place at an average rate of 1.5-2 MIGD. Hence, the total quantity of groundwater that had been produced in the field at the end of the year 1976 was ~8.4 billion IG. The current annual production is at a rate of ~275,000 IG (Alhumoud and Al-Ruwaih, 2015). The fresh groundwater body is concentrated along the central part of the field and surrounded and underlain by brackish to salty water. The Al-Rawdhatain field is situated in an elongated interior basin, extending over ~4-5 km from East to west and over ~15 km from North to South (Fig. 2). In 1963, 26 production water wells were drilled of which 14 wells are still in use. The other 12 wells were shut down due to the increase in the salinity of the groundwater. The field production has decreased over time while the salinity increased and ranged between 295 and 3560 mgL^{-1}.

Climate: Kuwait is a typical semitropical intercontinental area. The climate is extremely hot and dry in the summer and mild to cold in the winter. Rainfall is scarce and limited to the period from October to May. The annal precipitation has fluctuated during the period of 1962-2018. It reached its maximum value of 320 mm in 2018 and the minimum value of 25 mm was recorded in 1991. The 56 year average of the total precipitation is 131.5 mm (Alhumoud and Al-Ruwaih, 2015; Alhumoud, 2008).

Corresponding Author: Jasem M. Al-Humoud, Department of Civil Engineering, College of Engineering and Petroleum,
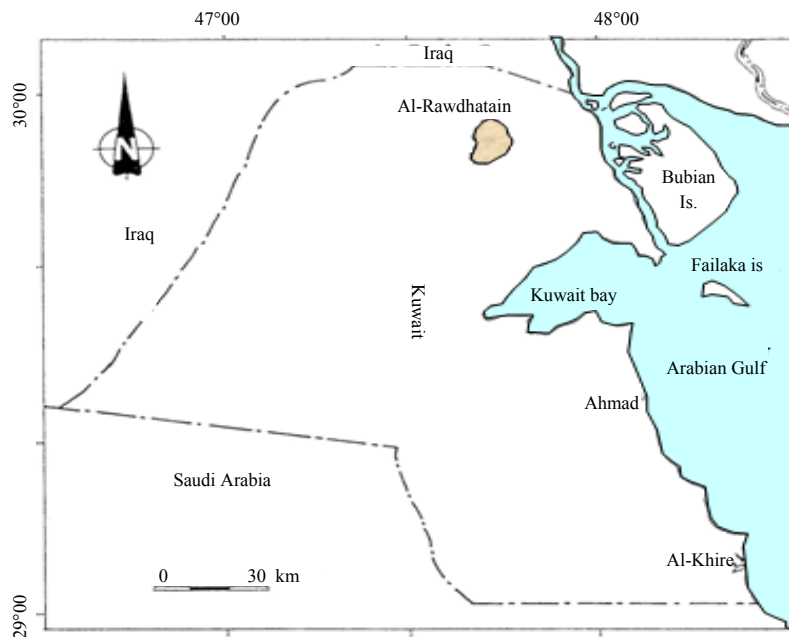Kuwait University, Kuwait, Kuwait
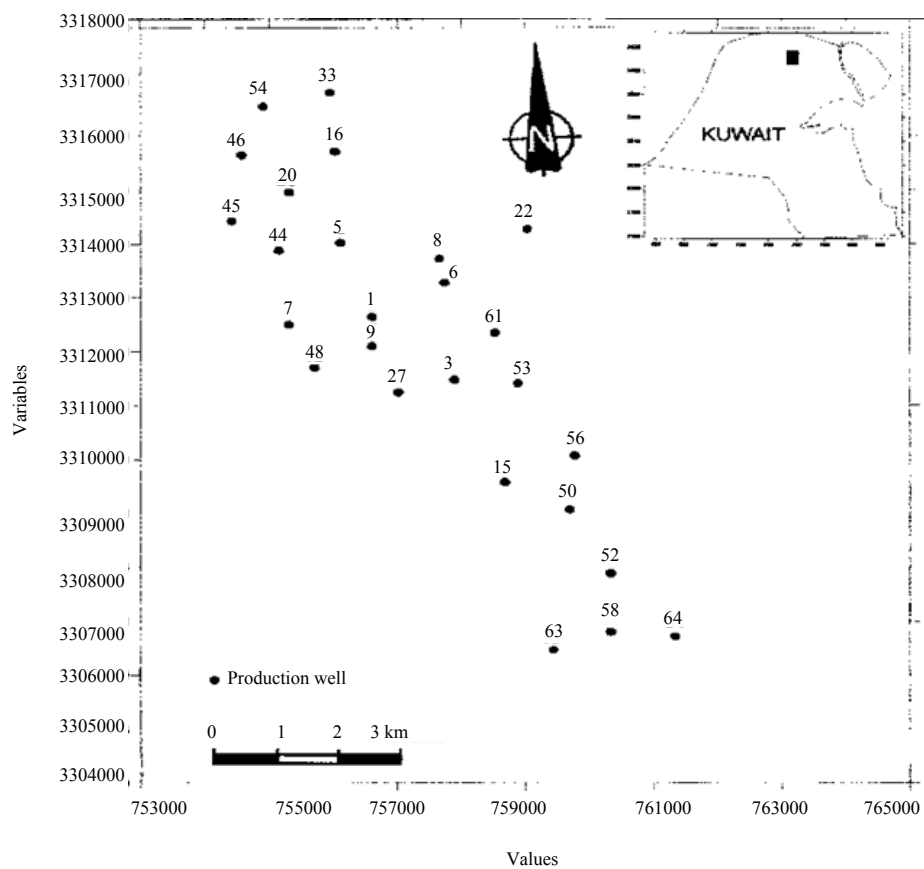
Fig.1: Location of the study area

Fig. 2: Location of the water wells in the Al-Rawdhatain field

Evaporation greatly dominates throughout the year; it increases in the summer because of high temperatures and high wind speeds and decreases in relative humidity. The very low average annual precipitation, high rate of evaporation and dry sandy nature of the top soil are the main causes of the scarcity of natural water resources. Therefore, the main natural water sources in Kuwait are limited to the brackish groundwater.

Geology of Kuwait

Topography: The state of Kuwait is located at the head of the Arabian Gulf. The topography of Kuwait is generally, flat with a gentle rise from the sea level at the coast to an elevation of ~270 m in the South Western corner of the country. The landscape of Kuwait is characterized by a low relief desert with a, generally, featureless, gently undulating ground surface covered with sand and gravel. The main features are the Jal Az-Zor escarpment, Ahmadi ridge, Wadi Al-Batin and Wara hill. The Jal Az-Zor escarpment which is located in the North of Kuwait Bay is ~60 km long and has an elevation of 145 m above sea level. The Ahmadi ridge is located in the East parallel to the coastline South of Kuwait city. It has an elevation of ~137 m above mean sea level. Wadi Al-Batin is a valley along the Western border; it is 8-11 km long and has a relief of 70 m. The central part of Kuwait and the neutral zone are featureless with few wadis and little vegetation. The coast is situated in the East of the country and sabkha (salty marshland) has developed along the coast. In the Northeastern part of the country, a few barchan dunes are observed up to 25 m (Omar *et al*., 1981; Al-Sulaimi and Al-Ruwaih, 2005; Al-RUWAIH *et al*., 2012).

General stratigraphy: The stratigraphical column of Kuwait was mainly influenced by the stable shelf condition of the Arabian plate, causing the deposition of shallow water sediments and evaporates. The land surface was formed by sedimentary rocks and sediments ranging from Middle Eocene to the current period. The Dammam Formation represents the oldest exposed sedimentary rocks. Recent deposits of fine-grained beach sand cover the Southern coast of Kuwait and the neutral zone. The Cenozoic (Tertiary-Quaternary) sediments can be divided into two groups: the Kuwait and Hasa groups (Fig. 2). The Mesozoic (Late Cretaceous) sediments are characterized by carbonate rocks (Al Sharhan and Nairn, 1997; Al-Ruwaih, 2001; Al-RUWAIH *et al*., 2012).

A marked erosional unconformity surface separates the Kuwait group from the underlying Hasa group. The Hasa group mainly consists of carbonate rocks is partly dolomitized in the lower parts and composed of anhydrite in the middle parts. The Hasa group consists of three formations that range in age from Middle Eocene to Paleocene and in descending order are the Dammam,

Rus and Radhuma formations (Alhumoud *et al*., 2010). The Hasa group underlies the whole state of Kuwait. It consists of soft porous chalky limestone and hard crystalline dolomitic limestone and green shale at the base. The Dammam Formation gently dips towards the North and Northeast. The Dammam Formation aquifer is isolated by confining layers. However, where these layers are absent, the Dammam Formation aquifer comes into direct contact with the underlying Radhuma aquifer and the overlying Kuwait group aquifer. Anhydrites of the Rus Formation act together with the basal shale of the Dammam Formation as an aquitard, separating the underlying Radhuma aquifer from the Dammam Formation aquifer. Based on the lithology, hydraulic properties and karstification, the middle part of the Dammam Formation represents the main aquifer in Kuwait (Al-Sulaimi and Al-Ruwaih, 2004). The thickness of the Dammam Formation aquifer varies from 120 m in the South Western corner of the country to 280 m in the Sabriya area in the North. The Damamm aquifer has a thickness of ~225 m in the synclinal area West of the Ahmadi ridge and >350 m East of it (Fig. 3).

The aquifer system in Kuwait: The most significant aquifer in Kuwait is the Tertiary-quaternary system. Between the early 1950's and early 1970's, two separate aquifers were identified based on the gross lithology. These aquifers are the upper clastic sediments of the Kuwait group and lower Dammam Formation which are separated by a confining layer of cherts and/or clay (Al-Ruwaih *et al*., 2005). The Eocene aquifer system which starts in the Dahna area in Saudi Arabia, consists of two limestone formations that is the Radhuma and Dammam formations. These two formations are separated by the anhydrite-bearing rus formation. This aquifer system is regionally confined, except in its recharge outcrop area in Saudi Arabia and in the discharge areas of the Arabian Gulf coast. The recharge of the Dammam Formation aquifer occurs in the Southern Iraqi desert West of Kuwait and in Saudi Arabia (400 km from Kuwait) where the exposures of the Dammam Formation aquifer cover an area of 1200 km^2 (Tleel, 1973). However, this aquifer system was mostly recharged during ancient periods while the current recharge is weak. The lateral outflow is directed eastwards of the Arabian Gulf and North ward into Iraq (Mukhopadhyay *et al*., 1994). Discharge is indicated by terrestrial springs, upward leakage into the overlying aquifer and evaporation through coastal sabkhas. The salinity of the Dammam Formation aquifer increases from SW-N-NE from brackish (3000 mgL^{-1}) to brine (>150,000 mgL^{-1}). This increase in the salinity may be attributed to the geometries of the recharge and discharge of the aquifer system. In addition to the location of Kuwait at the edge
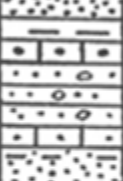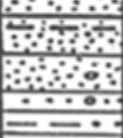
Age	Group	Formation	Graphic log	Lithology	Grand water conditions
Holocene				Beach sands sand gravel playa silts and clays, wadfi alluvium	Above ground-water saturation or locally contain brackish to saline water
Pleisto- cene	Kuwait group	Dibdibba		Coarse upland gravels Gravel and sand, mainly conglomeratic sandstone, siltstone shale, up to 120 m	Water locally fresh beneath wadis and depressions, brackish at depth
Pilocene					
Miocene		Lower fars		Fine to conglomeratic calcareous sandstone; sand variegated limestone, gypsiferous, 100 m thick	Water, generally, brackish
Oligocene		Undiffe-rentiated Fars and Ghar		Quartzose sandstone; sand and conglomeratic, some shale in lower part, few meters to 250 m thick	Groundwater is generally, brackish
				Unconformity surface	
Eocene	Hasa group	Dammam		Discontinous chert cap, chalky and siliceous limestone, dolomite, 200 m thick	Moderately permeable, moderately brackish water Southwest of Kuwait, very brackish in East and South
		Rus		Anhydrite limestone, marl 70-120 m thick	Brackish/saline water?
		Radhuma		Marly limeston, dolomite aqnhydrite, 180-400 m thick	Brackish/saline water?

Fig. 3: Lithostratigraphic representation of the tertiary-quaternary sediments of Kuwait (modified after Mukhopadhyay *et al*., 1994)

of the Arabian Plate in the Western Arabian Gulf synclinorium which hinders the groundwater movement and discharge. It might also be due to the decrease in the porosity and permeability along the SW-N-NE direction in addition to the long distance that the groundwater has to travel from the recharge to discharge areas (Talebi, 2003). The usable fresh groundwater (i.e., Total Dissolved Solids (TDS) content <1000 mgL^{-1}) in the Al-Rawdhatain field occurs in the upper part of the saturated sandstone beds of the Dibdibba Formation The water-bearing zones are represented by two aquifers.

The first aquifer has a saturated thickness ranging from 12-36 m and contains fresh groundwater in the depression. The effective thickness of the second aquifer varies from 11- to 18 m; it contains brackish water in the upper part and saline water in the lower part. The groundwater flows through the upper part of the first aquifer under water table conditions while it flows under artesian conditions in the lower part of the first well in the second aquifer. The depth to the initial water level ranges from 23-46 m depending on the land surface elevation (Hadi and Al-Ruwaih, 2008). Based on studies of the

Al-Rawdhatain depression conducted by the salinity ranges between 400-1500 mgL^{-1}. The fresh groundwater body is concentrated in the central part of the field. The study of the groundwater quality indicates a slight change in the salinity with time. The most notable change in the salinity occurs close to the borders of the field. The groundwater chemistry analysis indicates the presence of five groundwater chemistry types in 1981: sodium bicarbonate, calcium bicarbonate, sodium chloride, sodium sulphate and calcium sulphate. Hadi and Al-Ruwaih (2008) reported that the salinity of the aquifer ranges from 295-3560 mg/L^{-1} and that the chemical groundwater types include sodium bicarbonate, calcium bicarbonate, sodium chloride, sodium sulphate and calcium sulphate.

Objectives of this study: The main objectives of this study were the investigation and evaluation of the groundwater quality in the Al-Rawdhatain field to determine the prevailing geochemical processes in the aquifer, study the groundwater quality changes and trends during the period of 1985-2015, deduce the source rock and assess the chemical equilibrium of the groundwater with respect to the minerals of the aquifer matrix. In addition, the groundwater chemistry types and genesis were analyzed.

MATERIALS AND METHODS

In this study, geological and geochemical investigations were carried out on the Dammam Formation aquifer, mainly based on the chemical data collected from the Ministry of Electricity and Water (MEW) Kuwait in the Al-Rawdhatain field in the period of 1985-2017. The chemical analyses of the major ions in the groundwater such as Ca^{2+}, Mg^{2+}, Na^{+}, K^{+}, HCO$_{3-}$, SO$_4^{2-}$ and Cl^{-} were expressed in mg/l and converted to equivalent per million (e.p.m.) by multiplication with an appropriate conversion factor based on mathematical equations (Fetter, 1994). Subsequently, the %epm. was calculated. The ion balance equation was applied to determine the accuracy of the chemical analyses (+5% is acceptable). In well-known graphical methods such as those introduced by Durov (1984) and Sulin (1948), diagrams are used to plot the chemical data to determine the groundwater chemistry types, genetic groundwater types and prevailing geochemical processes. Several computer programs have been utilized: the WATEQ4F program to compute the saturation indices of the minerals with respect to a certain water composition, the WATEVAL program (Hounslow, 1995) to deduce the source rock, surfer for windows to construct contour maps to visualize the distribution of the salinity, the SPSS program for the statistical analyses of various hydrochemical characteristics, the AQUACHEM package

to carry out graphical and numerical analyses of geochemical data and the Trend-Y-tector application for the trend analysis of the TDS in the study area.

Groundwater chemistry: During the field and laboratory analyses of 72 groundwater samples from the Al-Rawdhatain field, basic cations and anions such as Calcium (Ca^{2+}), Magnesium (Mg^{2+}), sodium (Na^{+}), potassium (K^{+}), Chloride (Cl^{-}), Sulfate (SO$_4^{2-}$) and bicarbonate (HCO$_{3-}$) were analyzed (Table 1). In addition, the temperature (°C), electrical conductivity (EC; μS/cm^{-1}) at 25°C and pH were determined. The chemical analysis data expressed in mgL^{-1} were converted to EPM and % (e.p.m.) to compare the data with analyses based on different methods. Table 1 shows that the EC, TDS and Na, gradually, increase over the years. This is a clear indication that the salinity in the Al-Rawadhatain field increases. Field analyses of the pH, EC, alkalinity and temperature are usually carried out immediately when the sample is collected using portable equipment. The chemical analyses should represent in situ aquifer conditions. Several constituents, especially, those involved in carbonate and redox reactions, undergo changes upon reaching the atmosphere. Redox changes lead to difficulties such as the precipitation of metals, thus, the samples must be stabilized to keep the metal ions in solution (Hunt and Wilson, 1986; Vanloon and Barefoot, 1989).

The groundwater chemistry types are displayed in Table 2. The table shows that the groundwater in the study area was mainly dominated by Na$_2$SO$_4$, followed by NaHCO$_3$, CaSO$_4$ and Ca (HCO$_3$)$_2$, during the entire study period (1975-2015). This reflects that simple dissolution and mixing are geochemical processes occurring in the aquifer. The ion balance equation was used to validate the hydrochemical analyses of standard inorganic constituents (+5% is acceptable):

$$\text{Charge balance} = \left(\sum \text{cations} - \sum \text{anions} \right) / \left(\sum \text{cations} + \sum \text{anions} \right) \times 100$$

where all values are expressed in milliequivalents per Liter (meq/L). The charge balance analysis was applied to cations including Ca^{2+}, Mg^{2+}, Na^{+} and K^{+} and anions including SO$_4^{2-}$, Cl^{-} and HCO3^{-}.

Groundwater chemistry in the Al-Rawdhatain field (1985-2015)

Piper's trilinear diagram: The trilinear plotting technique developed was used to classify the groundwater based on the chemistry and compare chemical trends among different aquifer systems to determine the water quality. Piper's trilinear diagram is an effective tool for the segregation of the analysis data for critical studies with respect to the sources of the dissolved constituents in

Table 1: Chemical analysis of samples from the Al-Rawdhatain field (1975-2015)

Well No.	EC ($\mu s/cm^{-1}$)	pH	TDS (MgL^{-1})	Na (mgL^{-1})	K (mgL^{-1})	Ca (mgL^{-1})	Mg (mgL^{-1})	Cl (mgL^{-1})	SO$_4$ (mgL^{-1})	HCO$_3$ (mgL^{-1})	Groundwater chemistry types
1	494	7.9	360	63	3.9	47	13	51	120	151	NaHCO$_3$
5	738	7.9	564	105	4	57	11	59	230	161	Na$_2$SO$_4$
7	2023	8	1729	435	5	101	19	372	610	151	Na$_2$SO$_4$
9	655	8.1	464	97	3.9	52	12	88	140	171	NaHCO$_3$
15	1428	7.8	1223	200	3.9	142	31	221	430	161	Na$_2$SO$_4$
16	1273	8	1002	255	3.3	57	15	167	380	171	Na$_2$SO$_4$
20	1488	8	1131	315	3.3	49	10	249	385	166	Na$_2$SO$_4$
27	1273	8	1014	255	3.7	68	8	137	430	185	Na$_2$SO$_4$
44	1190	8	920	245	3.2	55	12	151	365	185	Na$_2$SO$_4$
1980											
1	650	7.9	419	40	3.5	59	12	48	69	171	Ca(HCO)$_3$
3	1600	7.9	1130	120	4.5	144	27	133	400	145	CaSO$_4$
5	1010	7.9	662	90	3.5	73	10	68	216	172	Na$_2$SO$_4$
6	1544	7.7	767	125	4.9	98	12	84	248	203	Na$_2$SO$_4$
9	1397	8.1	664	131	5.1	69	12.4	150	194	145	Na$_2$SO$_4$
15	1617	8.05	871	110	3.6	99	25	155	168	205	NaHCO$_3$
16	1660	7.95	1080	255	4	61	7.5	175	368	167	Na$_2$SO$_4$
20	2460	7.95	1600	410	5	46	9	368	436	155	Na$_2$SO$_4$
27	1838	8.2	952	220	4	71	12.4	98	416	172	Na$_2$SO$_4$
58	1544	8.2	754	108	5.1	97	13.5	93	250	192	Na$_2$SO$_4$
61	1382	8.1	674	134	4.7	66	12.4	96	209	167	Na$_2$SO$_4$
64	2279	8.2	1378	265	4.3	94	15.5	281	376	162	Na$_2$SO$_4$
1985											
1	650	7.8	391	55	5	52	12	52	72	169	NaHCO$_3$
3	1978	7.5	1737	190	6.5	252	31.2	212	713	129.8	CaSO$_4$
5	904	7.7	614	100	4.5	72.4	8.4	58	225	188	Na$_2$SO$_4$
6	1182	7.8	790	115	5	100	12	84	270	187	Na$_2$SO$_4$
9	927	7.6	670	105	4.5	75.6	11.2	118	168	140.8	Na$_2$SO$_4$
15	1638	7.7	1177	168	4.2	160	26	241	375	166	Na$_2$SO$_4$
16	1413	7.8	946	218	3.1	52.4	7.6	128	341	179	Na$_2$SO$_4$
20	2034	7.8	1504	410	3	69	9.6	324	440	172.2	Na$_2$SO$_4$
27	1526	7.7	1165	255	5	90	14.4	152	375	165.4	Na$_2$SO$_4$
44	1543	8.4	1154	300	3.2	51.9	7.2	244	304	145	Na$_2$SO$_4$
58	678	7.6	560	30	4	91	12	52	108	204.9	Ca(HCO$_3$)$_2$
61	1252	8.5	965	240	3	42.6	5.8	128	264	163	Na$_2$SO$_4$
1990											
1	375	7.9	305	16	3.6	47	8	9.4	38	146	Ca(HCO$_3$)$_2$
3	1100	7.8	862	130	5.9	126	16	133	316	142	Na$_2$SO$_4$
5	786	7.8	542	98	4.7	63	8	41.6	176	183	NaHCO$_3$
6	855	7.65	658	106	5.4	105	12	77	256	182	Na$_2$SO$_4$
7	3850	7.6	2902	740	8	212	40	813	986	101	Na$_2$SO$_4$
9	989	7.7	686	119	5.7	90	12	127	206	128	Na$_2$SO$_4$
16	1187	7.8	976	245	3.5	58	8	138	316	168	Na$_2$SO$_4$
20	2090	7.9	1396	430	3.6	68	10	370	450	161	Na$_2$SO$_4$
27	782	7.8	554	102	5.3	77	10	90.3	172	153	Na$_2$SO$_4$
44	1671	8	1212	373	3.6	44	8	304	405	154	Na$_2$SO$_4$
58	1313	7.65	650	52	4.8	120	16	83	180	174	CaSO$_4$
61	1148	8.1	902	265	3.6	41	6	130	328	190	Na$_2$SO$_4$
64	2279	8.2	1378	265	4.3	94	16	281	376	162	Na$_2$SO$_4$
1995											
1	538	8.09	356	59.1	0	50	7	40	90	164.5	NaHCO$_3$
5	1076	8.02	684	148	0	68	11	119	240	157.6	Na$_2$SO$_4$
6	1209	7.9	832	114	0	125	17	140	276	177.6	CaSO$_4$
7	4520	7.98	3224	708	0	264	52	853	1186	97.6	Na2SO$_4$
9	818	8.22	580	77.7	0	82	11	85	173	129.3	CaSO$_4$
20	2070	8.24	1308	377	0	53	7	314	445	176.7	Na$_2$SO$_4$
2000											
1	463	8.1	324	50	4.6	32	19	69.6	76.5	124.9	NaHCO$_3$
3	2250	7.4	1684	213	10	210	52	259	712	105.5	Na$_2$SO$_4$
6	960	8	632	92	6.5	69	29	131	213	116	Na$_2$SO$_4$
16	1350	7.9	904	240	4.9	22	18	132	312	167	Na$_2$SO$_4$
61	1358	8	910	259	5.1	24	17	112	325	183.9	Na$_2$SO$_4$
2010											
3	2318	7.4	1280	190	6	255	27.4	225	581	130	CaSO$_4$
7	4879	7.6	2830	450	8	260	46.1	445	1000	101	Na$_2$SO$_4$
20	2045	7.8	1120	185	3	52.9	9.71	149	157	172	NaHCO$_3$
27	2445	7.6	1360	168	5	133	133	441	539	174	Na$_2$SO$_4$
58	1498	7.6	813	100	4	86.9	19.2	139	162	147	Na$_2$SO$_4$

Table 1: Continue

| 2012										
1	1154	8.1	935	85	4	81	23	155	192	102	Na$_2$SO$_4$
3	2306	7.7	1868	200	6	254	33	276	820	87.24	CaSO$_4$
20	1699	8.4	1376	376	4	35	12	268	351	121.3	Na$_2$SO$_4$
27	2799	7.8	2267	250	4	232	42	42	626	410	Na$_2$SO$_4$
44	2067	8.4	1674	380	4	36	12	344	470	87	Na$_2$SO$_4$
2015										
1	516	8	950	165	3	118	9.8	173	380	100	Na$_2$SO$_4$
15	1739	7.9	3210	391	5	288	34.2	602	750	128	Na$_2$SO$_4$
20	1847	7.9	1532	267	3	48	3	363	100	124	NaHCO$_3$
27	2804	8.7	2110	415	5	256	24.4	623	700	84	Na$_2$SO$_4$
44	2265	8.1	2500	514	3	66	15.6	142	460	108	Na$_2$SO$_4$
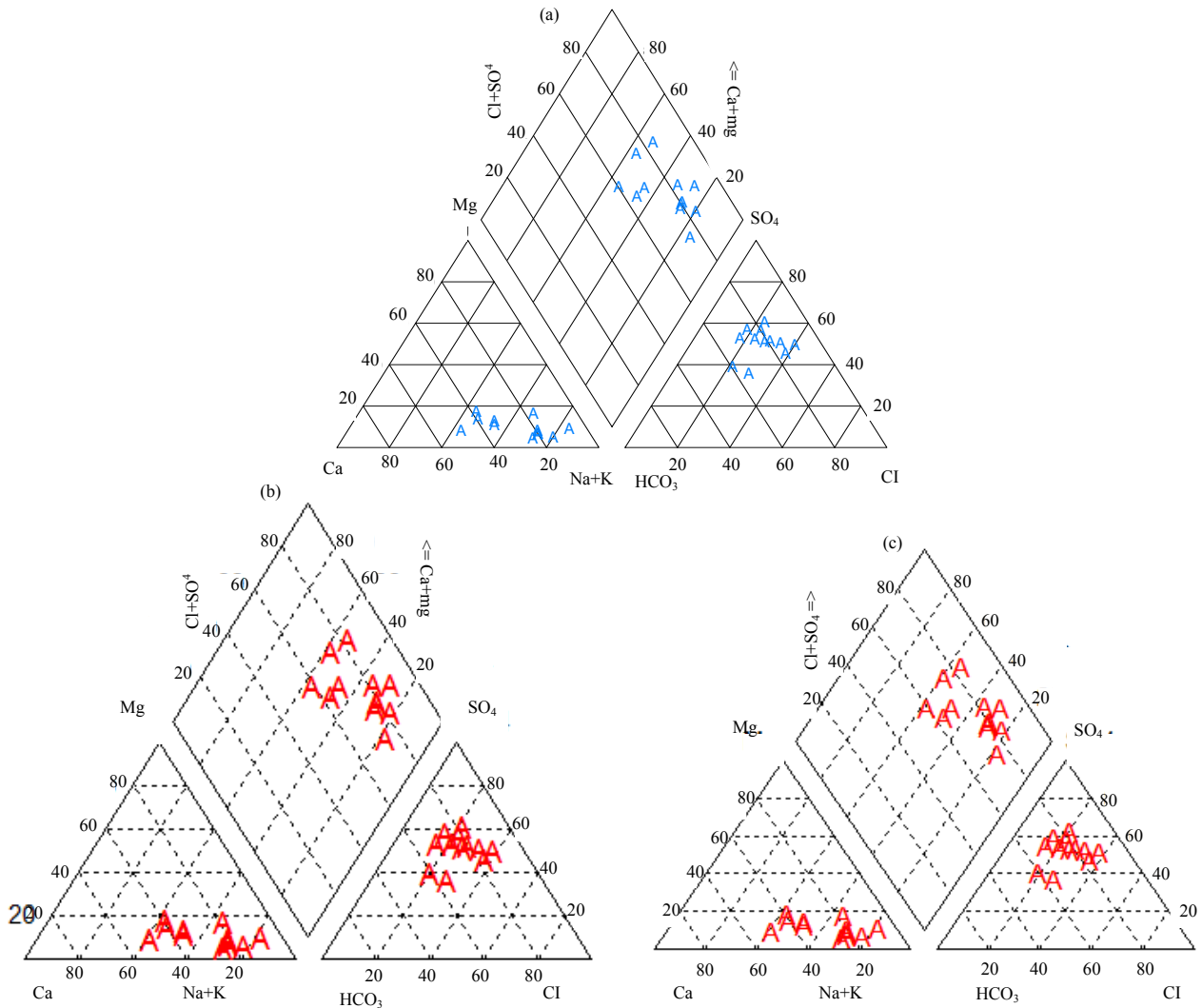
Fig. 4: Piper diagram for the Al-Rawdhatain field (a) 1985-1994 (b) 1995-2004 and (c) 2005-2015

the groundwater, modifications in the characteristics of the water as it passes through an area and related geochemical problems.

The piper diagram was utilized to plot the chemical analysis data of the Al-Rawdhatain field for the period of 1985-2015 (Fig. 4). The piper diagrams shows that most of the groundwater samples from t he Al-Rawdhatain field during the study period plot in the subareas 1, 4 and 9 in which alkaline earths (Ca^{2+}, Mg^{2+}) exceed alkalis (Na$^+$+ K$^+$), strong acids exceed weak acids and the

Table 2: Groundwater chemistry types in percentage (1975-2015)

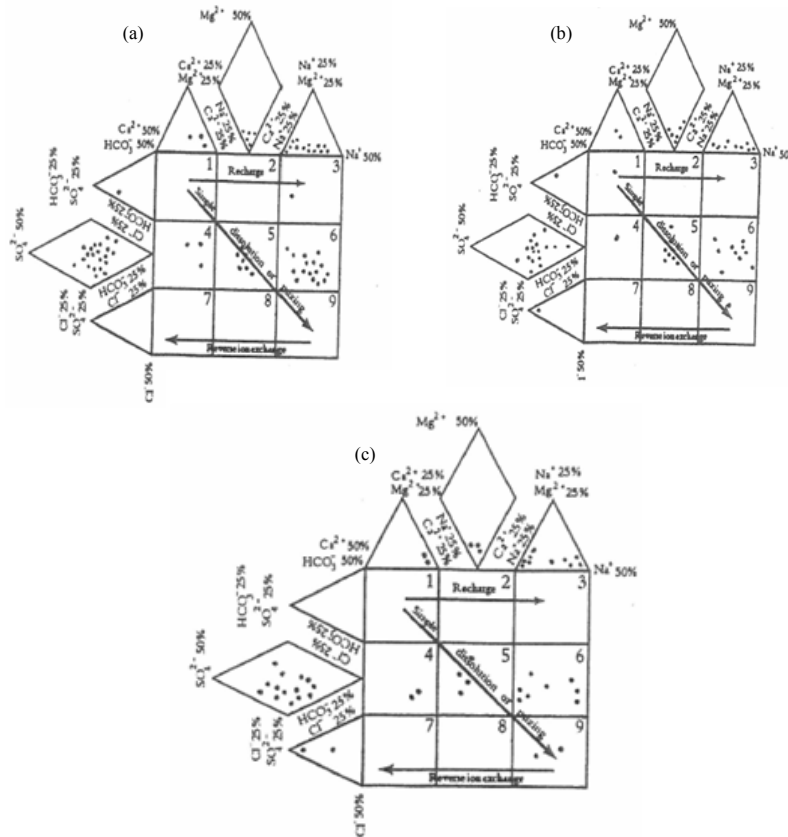| Chemical type	1975-1985	1986-1997	1998-2015
Na_2SO_4	75.75	70.8	73.33
$NaHCO_3$	12.12	12.5	13.33
$CaSO_4$	6.06	12.5	13.33
$Ca(HCO_3)_2$	6.06	4.16	0

Fig. 5: Expanded Durov diagram of the Al-Rawdhain field (a) 1985-1994 (b) 1995-2004 and (c) 2005-2015

non-carbonate hardness (secondary salinity) exceeds 50%, respectively. A few groundwater samples plot in the subareas 2 and 7 in which the alkalis exceed alkaline earths and the non-carbonate hardness/alkalis (primary salinity) exceeds 50%, respectively. In addition, it shows that the strong acids exceed weak acids and none of the cation-anion pairs exceed 50%. Therefore, the chemical analyses show that the groundwater properties in the study area are dominated by alkalis and strong acids.

Expanded Durov diagram: The groundwater samples of the Al-Rawdhatain field have been plotted on the expanded Durov diagram (Durov, 1948) in Fig. 5 for the periods of 1985-1994, 1995-2004 and 2005-20015. Several groundwater samples are located in area 5 which indicates simple dissolution or mixing processes of the groundwater. However, the residual samples are located in area 8 which indicates that the Cl⁻ ion is dominant and

dominant cations are absent. This suggests that reverse ion exchange of Na^+-Cl^- water is the prevailing chemical process.

The chemical data reveal that the groundwater samples are grouped according to the subsidiary processes such as a cation exchange and simple dissolution or mixing. Most of the ground water samples are distributed among the subareas 4, 5 and 6. The composition of the groundwater in subarea 4 shows the dominance of Ca^{2+} and SO_4^{2-} which indicates recharge water or mixed water. The groundwater samples in subarea 5 show no dominant anions or cations, indicating simple dissolution or mixing. The majority of the samples located in subarea 6 are dominated by SO_4^{2-} and Na and mixing influences the aquifer chemistry.

Sulin's classification graph: Sulin's graph (Sulin, 1948) was prepared for the genetic classification of water. The graph is divided into two main quadrants depending on
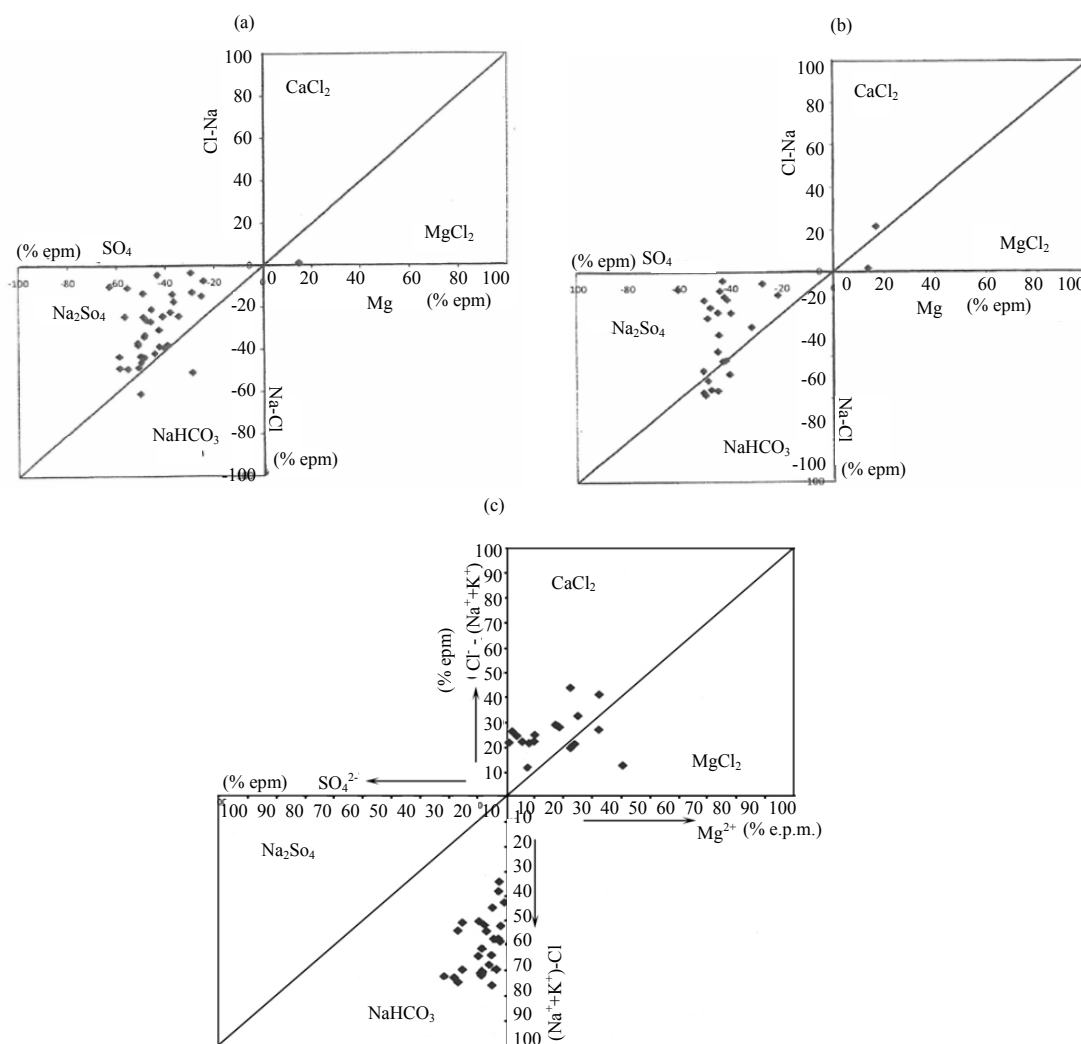
Fig. 6: Sulin's classification of Al-Rawdhatain field (a) 2001-2005 (b) 1995-2004 and (c) 2005-2015

the Na^+/Cl^- ratio. Water with a ratio of Na^+/Cl^- >1 is located in the lower quadrant whereas water with a Na^+/Cl^- ratio <1 is located in the upper quadrant. A diagonal line with a Na^+/Cl^- ratio of 1 separates the two quadrants into four equal triangles, each corresponding to a different genetic water type while the coefficients $(Na^+-Cl^-)/SO_4^{2-}$ and $(Cl^--Na^+)/Mg^{2+}$ are used to identify each type of genetic water. The upper quadrant contains the chloride group with Cl-Mg and Cl-Ca genetic types reflecting marine conditions as an origin of formation whereas the lower quadrant contains the Na^+ group with the $Na-SO_4$ and $Na-HCO_3$ genetic types (terrestrial condition) reflecting the continental origin of groundwater formation. Sulin's concept has been applied to the data of rge Al-Rawdhatain field for the study period (Fig. 6). The groundwater samples of the study field present two groundwater genetic types: $Na-SO_4$,

$Na-HCO_3$. The majority of the groundwater samples shows that the $Na-SO_4$ water type represents continental terrestrial water which suggest that the groundwater is of meteoric origin, originating from infiltration. Few samples indicate the Cl-Mg water type which represents a marine environment and evaporate sequences (Al-Ruwaih *et al.*, 2005; Salman *et al.*, 2019). Therefore, it is suggested that most of the $MgCl_2$-type water has been replaced by Na_2SO_4-type water of atmospheric origin by recharge processes.

Geochemical modeling: Geochemical models were used to estimate the chemical reactions in the groundwater system such as dissolution and precipitation of solids, ion-exchange and sorption by clay minerals (Talebi, 2003; Marandi and Shand, 2018). Based on Plummer (1994), the geochemical models can be divided into two general

types. The first type refers to forward models and the second type refers to inverse models. The aim of the forward model is to predict the water compositions and mass transfers resulting from hypothesized reactions (Plummer *et al*., 1994). The inverse geochemical model deduces the chemical changes that take place as water evolves along a flow path (Plummer *et al*., 1994). The typical inverse modeling approach groups speciation and mass balance models (Parkhurst and Plummer, 1993).

In this study, the inverse speciation model was applied to determine the thermodynamic speciation calculations of the groundwater in the study area for the periods of 1985-1994, 1995-2004 and 2005-2015 (Table 3) using the WATEQ4F program (Ball and Nordstrom, 1992) to determine the degree of saturation of the groundwater with respect to certain minerals. In addition, a mass balance model using the WATEVAL program proposed by Hounslow (1995) was applied to deduce the source rock to investigate the major geochemical processes that influence the groundwater chemistry of the Al-Rawdhatain field.

Speciation modeling: The saturation state of the water is an important concept because it can be used to better understand the chemical history of the groundwater. The saturation state of any solution with a specific mineral phase can be calculated as follows (Plummer *et al*., 1994):

$$SI = \log\left(IAP/K_{sp}\right) \tag{1}$$

Where:
SI : Saturation Index
IAP : Ion Activity Product and
K_{sp} : Solubility product

If SI>0, the solution is saturated with the mineral and precipitation is possible. If SI<0, the solution is under saturated with the mineral and dissolution occurs. If SI = 0, the solution is in equilibrium with the specified mineral.

Langelier index: The Langelier index is the Saturation Index (SI) for calcite. Any solution containing Ca^{2+} and CO_3^{2-} has an IAP = $[Ca^{2+}]$ $[CO_3^{2-}]$. In the case of calcite the SI may be expressed in a different manner (Table 3):

$$SI = pH_{of\ solution} - pH_{at\ which\ calcite\ precipitates} \tag{2}$$

Usually known as Langelier index. Thus, the Langelier index is SI (calcite) = log IAP/K_{sp} = $pH_{of\ solution}$-$pH_{at\ which\ calcite\ precipitates}$. If the Langelier index is positive, the solution is oversaturated with respect to calcite; if it is negative, it is undersaturated with respect to calcite (Hunslow, 1995; Wunsch *et al*., 2018). The degree of saturation or undersaturation of groundwater with

respect to some minerals has been calculated for the Al-Rawdhatain field for the periods of 1985-1994, 1995-2004 and 2005-2015. The results of the thermodynamic speciation calculations are shown in Table 1. In the period 1985-1994, the groundwater shows a negative saturation index for anhydrite, gypsum and halite which demonstrates that the groundwater was undersaturated with respect to these minerals. On the other hand, the saturation index of calcite and dolomite shows positive index values which means that the groundwater was oversaturated with respect to calcite and dolomite. The average partial Pressure of Carbon dioxide (PCO_2) of the groundwater for this period is 3.11×10^{-3} atm which is greater than the PCO_2 of the Earth's atmosphere (5.0×10^{-3}) and reveals that the aquifer contains carbon dioxide in the soil zone.

In the period of 1995-2004, the groundwater shows a negative saturation index for anhydrite, gypsum and halite which reveals that the groundwater was undersaturated with respect to these minerals. However, calcite and dolomite have a positive saturation index, which proves that the groundwater was over saturated with respect these minerals and indicates the precipitation of calcite and dolomite. The average partial pressure of CO_2 equals 1.86×10^{-3} atm which is greater than the PCO_2 of the Eart's atmosphere. The results of the saturation index for anhydrite, dolomite, gypsum and halite for the period of 2005-2015 indicate that the groundwater was undersaturated with respect to these minerals while the groundwater was oversaturated with respect to calcite which might have precipitated. The calculated mean value of PCO_2 is 1.98×10^{-3} atm suggesting a deep, closed environmental system. Table 4 summarizes the mean saturation indices and the PCO_2 values of the Al-Rawdhatain field. Generally, the groundwater exhibits an oversaturation with respect to calcite and dolomite and undersaturation with respect to anhydrite, gypsum and halite. The PCO_2 ranges between 3.95 and 5.65×10^{-3} atm which is greater than the PCO_2 of the Earth's atmosphere ($10^{-3.5}$ atm); this might indicate that the groundwater was charged with CO_2 during the infiltrating process through the soil zone, representing a deep closed environmental system (Appelo and Postma, 1994; Stigter *et al*., 1998; Hadi and Al-Ruwaih, 2005; Kalhor *et al*., 2018).

Source rock deduction: A mass balance technique using the WATEVAL program (Hounslow, 1995) was utilized to deduce the source rock of the Dammam Formation aquifer of the Al-Sulaibiya field to identify the main geochemical processes that influence the groundwater chemistry. The most common chemical reactions are gypsum dissolution, calcite precipitation, dedolomitization, ion exchange and silicate/carbonate weathering.

Hounslow's approach was applied to 72 groundwater samples of the Al-Rawdhatain aquifer; the pH values of

Table 3: Thermodynamic speciation calculations for the Al-Sulaibiya field (1985-2015)

Well No.	Ahydrite	Calcite	Dolomite	Gypsum	Halite	Pco$_2$ (×10^{-3})	Ionic strength
Period 1 (1985-1994)							
1	-1.64	0.24	0.19	-1.68	-7.07	1.80	0.09
3	-0.50	0.29	-0.06	-0.53	-6.04	3.57	0.03
5	-1.35	0.29	0.15	-1.38	-6.80	1.90	0.01
6	-0.91	0.46	0.46	-0.95	-5.44	1.32	0.03
7	-1.57	0.51	0.65	-1.60	-6.66	1.26	0.01
8	-0.86	0.49	0.60	-0.90	-5.98	2.27	0.02
9	-1.24	0.34	0.38	-1.27	-5.98	1.55	0.02
15	-1.31	0.26	0.10	-1.34	-5.73	1.50	0.02
16	-1.12	0.44	0.22	-1.16	-6.08	1.60	0.02
20	-1.26	0.37	0.35	-1.30	-6.05	1.69	0.02
22	-1.77	0.41	0.40	-1.80	-7.29	2.04	0.01
27	-1.36	0.63	0.67	-1.39	-5.75	5.05	0.02
44	-1.44	0.35	0.11	-1.48	-7.39	4.85	0.01
50	-1.46	0.71	0.83	-1.50	-6.12	4.52	0.02
52	-1.32	0.08	-0.28	-1.36	-5.45	1.76	0.03
56	-1.11	0.63	0.77	-1.15	-6.28	9.69	0.02
58	-1.34	0.56	0.67	-1.38	-6.49	1.21	0.01
61	-1.06	0.72	0.92	-1.10	-5.75	8.94	0.02
63	-1.17	0.46	0.31	-1.21	-6.96	3.20	0.01
Period 2 (1994-2004)							
1	-0.56	0.22	-0.26	-0.60	-6.01	4.55	0.03
3	-1.40	0.32	0.01	-1.43	-6.98	2.73	0.01
5	-1.09	0.39	0.11	-1.13	-6.69	3.35	0.02
6	-0.55	0.12	-0.21	-0.59	-4.9	2.14	0.06
7	-1.23	0.19	-0.22	-1.27	-6.42	2.37	0.01
8	-1.27	0.17	-0.25	-1.30	-6.09	2.47	0.02
9	-2.12	-0.74	-1.04	-2.16	-5.43	1.80	0.03
15	-1.34	0.32	0.02	-1.38	-6.63	2.26	0.01
16	-1.35	0.17	-0.14	-1.38	-5.57	1.39	0.02
20	-1.17	0.46	0.31	-1.21	-6.96	3.20	0.01
22	-1.41	0.36	0.16	-1.44	-6.07	1.38	0.2
27	-1.43	0.32	0.10	-1.47	-6.09	1.31	0.02
44	-1.71	0.52	0.45	-1.75	-7.20	1.23	0.01
50	-1.96	0.21	0.36	-1.99	-7.03	9.34	0.01
52	-1.25	0.48	0.36	-1.28	-5.56	9.87	0.03
56	-0.58	0.02	-0.29	-0.62	-5.90	3.69	0.03
58	-1.33	0.33	0.55	-1.36	-6.52	1.06	0.01
61	-1.68	-0.15	-0.11	-1.72	-6.11	1.95	0.02
63	-1.31	0.66	0.72	-1.35	-6.77	7.39	0.01
64	-1.64	0.02	0.16	-1.68	-6.15	1.70	0.02
Mean	-1.30	0.29	0.15	-1.34	-6.31	1.86	0.03
Period 3 (2005-2015)							
1	-0.56	0.22	-0.26	-0.60	-6.01	4.55	0.03
3	-0.43	0.22	-0.02	-0.47	-5.37	2.16	0.05
5	-1.54	0.20	-0.06	-1.58	-6.16	2.55	0.01
6	-0.81	0.28	0.30	-0.84	-6.29	3.93	0.02
7	-1.34	0.15	-0.08	-1.38	-6.45	3.43	0.01
8	-1.30	0.44	0.61	-1.34	-6.48	7.32	0.01
9	-0.46	0.29	-0.02	-0.49	-5.91	1.50	0.03
315	-1.49	0.37	0.54	-1.52	-5.62	4.23	0.02
16	-0.59	1.50	1.63	-0.63	-6.62	5.61	0.03
20	-1.39	0.20	0.19	-1.42	-5.51	2.99	0.03
22	-0.93	0.43	0.05	-0.97	-6.16	8.97	0.02
27	-0.49	0.69	0.84	-0.53	-5.29	1.34	0.04
44	-1.79	0.12	-0.70	-1.82	-5.62	1.44	0.02
50	-0.54	1.20	1.63	-0.58	-5.25	1.16	0.04
52	-1.16	0.27	0.18	-1.19	-5.77	7.58	0.03
Mean	-0.99	0.44	0.32	-1.02	-5.90	1.98	0.03

Table 4: Mean saturation indices and PCO$_2$ of the Al-Sulaibiya field

Study periods	Anhydrite CaSO$_4$	Calcite CaCO$_3$	Dolomite CaMg(CO$_3$)$_2$	Gypsum CaSO$_4$ 2H$_2$O	Halite NaCl	PCO$_2$
1985-1994	-1.24	0.42	0.33	-1.37	-6.30	3.11×10-3
1995-2004	-1.30	0.29	0.15	-1.34	-6.31	1.86×10-3
2005-2015	-0.99	0.44	0.32	-1.02	-5.90	1.98×10-3

the groundwater samples were determined and range from 7.4-8.7 with an average value of 7.92. This encourages the application of the mass balance technique to deduce the source rock of the Kuwait group aquifer of the Al-Rawdhata in field.

RESULTS AND DISCUSSION

Dissolution and precipitation: The progressive dissolution of minerals as groundwater moves down gradient in the aquifer results in an increase in the TDS content of the water. This effect is noticeable in sedimentary rocks because of the occurrence of highly soluble minerals such as gypsum, anhydrite and halite. The HCO_3^-/sum of anions ratio indicates the mineral dissolution rates in the aquifer.

The HCO_3^-/sum of anions ratio of all groundwater samples of the study area is <0.66 which suggests that gypsum and anhydrite are dissolving in the aquifer of the study area. This finding is supported by the results of the thermodynamic speciation calculations obtained previously where the mean values of gypsum range from -1.02 to -1.37 and anhydrite ranges from -0.99 to -1.30, respectively. Furthermore, calcite precipitation is a common process in aquifers. The chemical process is as follows:

$$Ca^{2+}_{(aq)} + CO_3^{2-}_{(aq)} \rightarrow CaCO_{3(s)} \qquad (3)$$
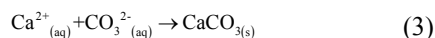
where $CaCO_3$ precipitates when $([Ca^{2+}][CO_3^{2-}]/K_{sp}) > 1$ and K_{sp} is the solubility product for calcite. Calcite precipitates when either Ca^{2+} or CO_3^{2-} increase such that the solubility product is exceeded or if the solubility product is reduced. Calcite also precipitates when the Ca^{2+} ion concentration increases by dissolving soluble calcium mineral such as gypsum $(CaSO_4 . 2H_2O)$. This process is called dedolomitization (Hounslow, 1995). The Langelier index which is an indication of calcite precipitation was computed for all groundwater samples of the study area during the selected study period and positive values ranging from 0-0.78 were determined, revealing that the groundwater is over saturated with respect to calcite which in turn might be precipitated in the system.

Dedolomitization: Dedolomitization may occur in aquifers containing limestone and dolostone. In its simplest form, dedolomitization is the replacement of dolomite by calcite according to the following reaction:

$$Ca^{2+}_{(aq)} + CaMg(CO_3)_{2(s)} \rightarrow 2CaCO_{3(s)} Mg^{2+}_{(aq)} \qquad (4)$$
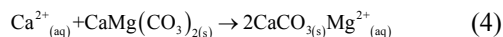
Back and Langmuir pointed out that the dedolomitization is a result of the dissolution of calcite, dolomite and gypsum and precipitation of calcite.
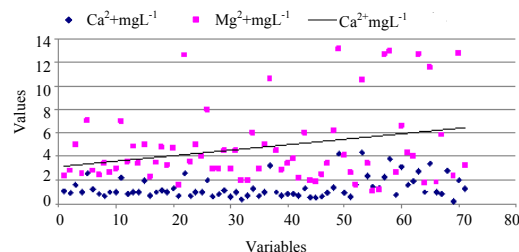

Fig. 7: Relationship between calcium and magnesium in the study area

The reaction is initiated by a Ca^{2+}/Mg^{2+} ratio >1. The high ratio of Ca^{2+}/Mg^{2+} is achieved by the introduction of dissolved gypsum or anhydrite into the aquifer. Richter and Kreitler suggested that dedolomitization is indicated by a ratio of $(Ca^{2+}+Mg^{2+})/SO_4^{2-}$ approaching 1. Based on the application of this concept to the study area, the calculated values of $(Ca^{2+}+Mg^{2+})/SO_4^{2-}$ for the groundwater samples are within the range of 0.8-1.2, revealing the occurrence of the dedolomitization process in the aquifer. Figure 7 shows systematic increases in the Mg^{2+} and Ca^{2+} concentrations, indicating dolomite and gypsum dissolution and calcite precipitation in the aquifer system. This may explain the saturation conditions with respect to calcite and slight undersaturation with respect to dolomite in the study area.

Cation exchange: The ratio $SiO_2/[(Na^+ +K^+)-Cl^-] < 1$ indicates the cation exchange in the aquifer. The results show that most of the groundwater samples of the study field fall within the range of cation exchange ratios below one. Thus, cation exchange occurs as one of the chemicals processes operating within the Kuwait group aquifer. Reverse ion exchange requires the presence of clay with exchangeable calcium and water higher in sodium than the clay exchange equilibrium concentration. Ion exchange can simply be represented by the following reaction:

$$2Na^+_{(aq)} + Ca\text{-}Clay \rightarrow Na_2\text{-}Clay + Ca^{2+}_{(aq)} \qquad (5)$$
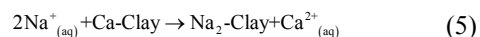
The result is often expressed in meq/L of $Na^+/Cl^- < 1$. However, most of the groundwater samples of the study area show $Cl^- > Na^+$, suggesting that reverse ion exchange likely occurs in the aquifer in the study period.

Weathering mode: Weathering is caused by the interaction of rocks with the atmosphere and hydrosphere. The HCO_3^{-1}/SiO_2 ratio indicates the dominant mode of weathering. Silica is not released by dissolving carbonate while silicate weathering releases a considerable amount of silica in the water. Hounslow (1995) reported that

Table 5: Major geochemical reactions in the Al-Rawdhatain field (1985-2015)

Chemical reaction	Index	Range	Percentage (%)
Carbonate weathering	HCO_3^-/SiO_2	>10	91.66
Albite	$Na^+/Na + Cl$	>0.5	88.88
Cation exchange	$SiO_2 < [(Na^+ + K^+) - Cl^-]$	<1	84.72
Plagioclase weathering	$Na^+ + K^+ - Cl^-$		
	$Na^+ + K^+ - Cl^- + Ca^{2+}$	>0.2 and <0.8	6.25
Calcite precipitation	Lagelier indices	Positive	57.69
Ion exchange	Na^+/Cl^-	<1	55.55
Dedolomization	$(Ca^{2+} + Mg^{2+})/SO_4^{2-}$	>0.8 and <1.2	31.94
Gypsum dissolution	$HCO_3/\text{sum of anions}$	<0.8	31.94
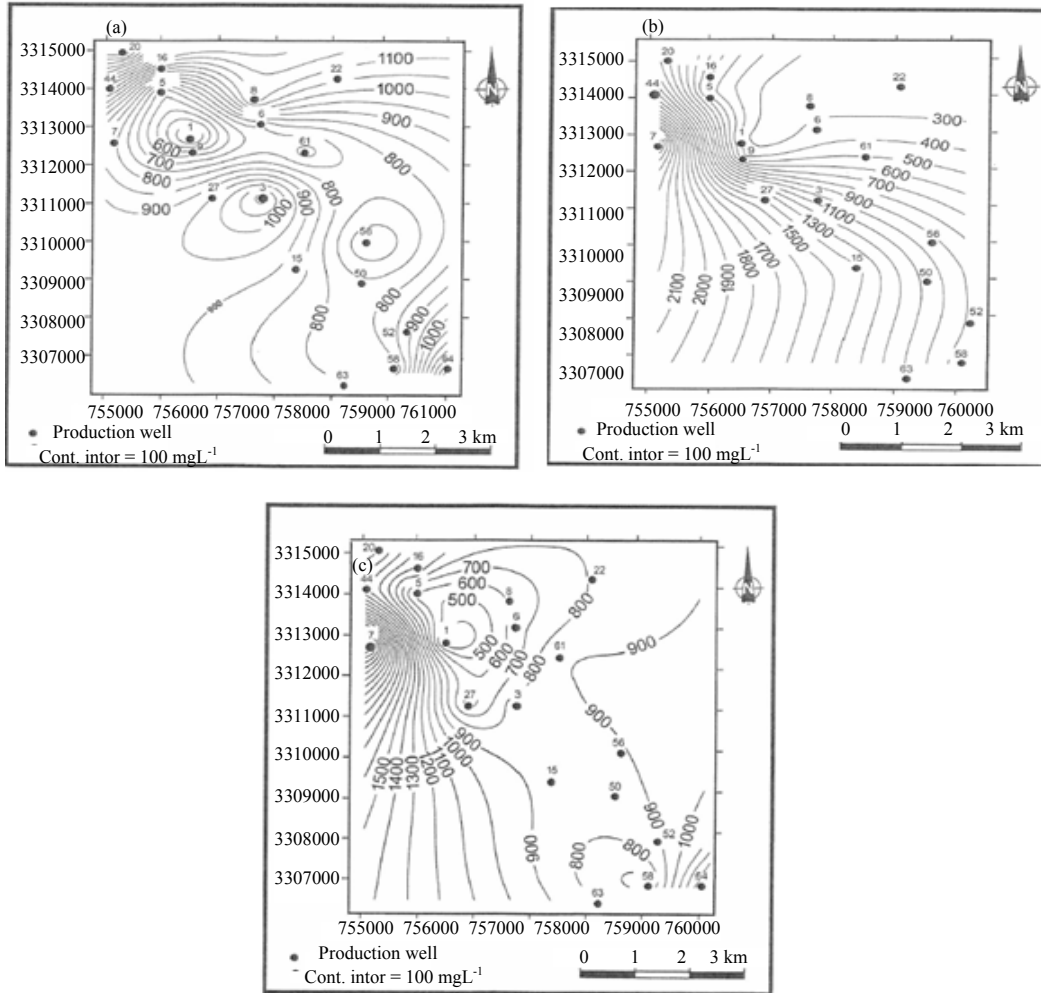
Fig. 8: Iso-salinity maps of the Al-Rawadhatain field (a) 1985-1994 (b) 1995-2004 and (c) 2005-2015

waters with $HCO_3^{-1}/SiO_2 < 5$ show dominantly silicate weathering while waters with $HCO_3^{-1}/SiO_2 > 10$ represent dominant carbonate weathering. Several groundwater samples in the study area have a ratio of $HCO_3^{-1}/SiO_2 > 10$, indicating carbonate weathering. Few groundwater samples represent silicate weathering because the HCO_3^{-1}/SiO_2 ratio is below 5. The remaining samples are ambiguous or uncertain. However, carbonate weathering is represented by 27% of the groundwater samples of the study field.

The groundwater of the Al-Rawdhatain field is dominated by carbonate weathering in the presence of silicate weathering. Gypsum and anhydrite are dissolving minerals in the aquifer of the study area. This is supported by the results of the thermodynamic speciation calculations obtained previously where the mean values of gypsum ranged from -1.02 to -1.37 and that of anhydrite ranged from -0.99 to -1.30. In addition, the calculated values for $(Ca^{2+} + Mg^{2+})/SO_4^{2-}$ for the
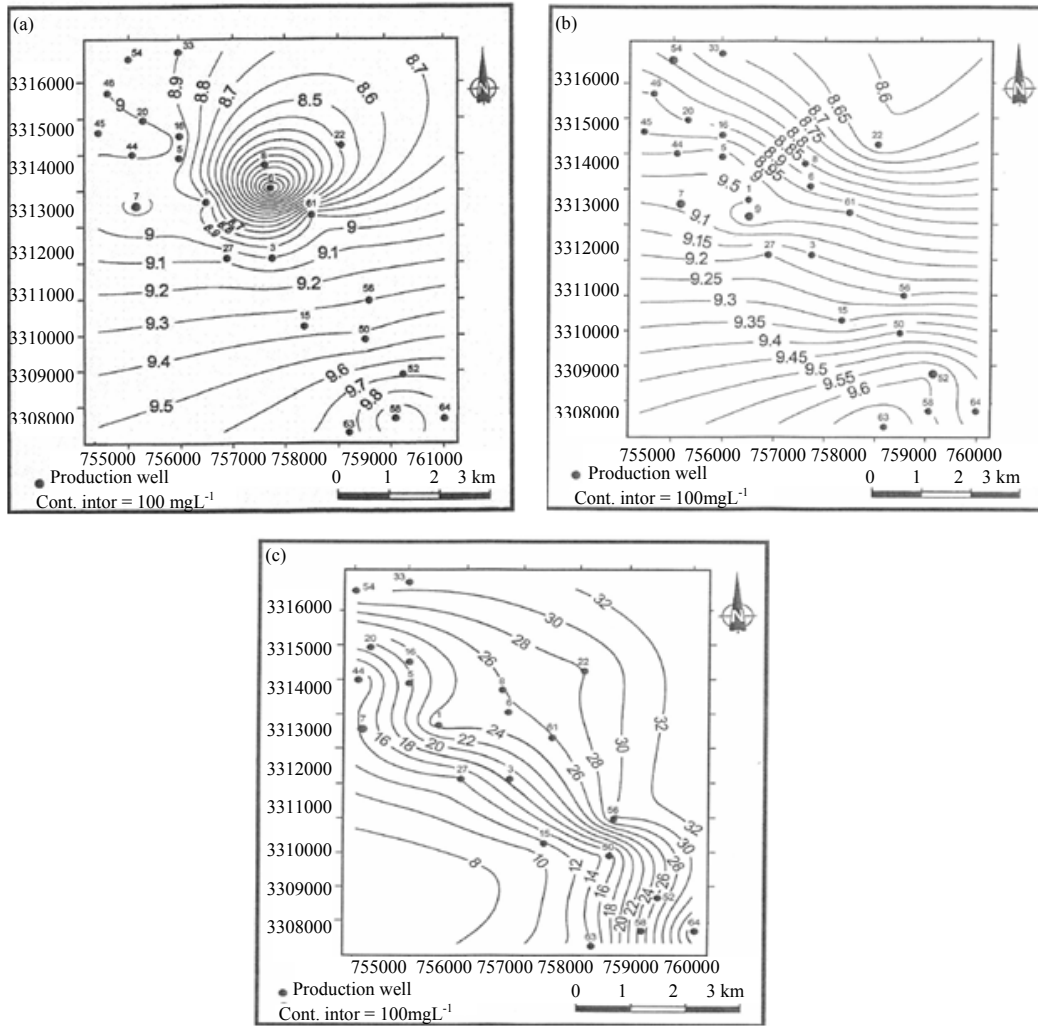
Fig. 9: Water levels in the Al-Rawdhatain field (a) 1985-1994 (b) 1995-2004 and (c) 2005-2015

groundwater samples ranged from 0.1-3.8 which is within the range of 0.8-1.2 where the dedolomitization process is involved in the aquifer. The cation exchange reaction appears to be one of the chemical processes operating within the Kuwait group aquifer. Table 5 summarizes the major geochemical reactions affecting the groundwater chemistry of the Dammam Formation aquifer in the study area.

Groundwater quality trends and water levels: The iso-salinity maps of the Al-Rawadhatain field were constructed for the different periods. Figure 8 shows that the fresh groundwater body is mainly concentrated in the central part of the field in contrast to the salinity which increases towards the periphery of the field. However, the areal distribution maps of the aquifer salinity reflect the morphology of the field which suggests that the groundwater is accumulated as lenses of freshwater in the Dibdibba Formation, the upper part of the Kuwait

group, surrounded by brackish groundwater. The salinity increased with time. It ranged from 530-1800 mgL^{-1} in 1966 from 400-1500 mgL^{-1} in 1995 and from 950-3210 mgL^{-1} in 2015. The water level considerably decreased in the Al-Rawadhatain field (Fig. 9). If we take well 22 as an example, the water levels in 1985, 1990, 2015 were 6, 8.65 and 28 m from the ground surface, respectively which clearly reflects the decrease in the water level and change in the aquifer storage. Accordingly, the MEW shows reduced field production to minimize the upward movement of the surrounding brackish groundwater and keep the fresh groundwater as a strategic reserve when natural resources are limited.

CONCLUSION

The aquifer system in Kuwait can be divided into two main aquifers that is, the Kuwait group and Dammam Formation aquifers. The Al-Rawdhatain field is one of the

main fresh groundwater resources in Kuwait. The total dissolved solids range from 305-2902 mgL^{-1}. The areal distribution of groundwater based on the TDS maps of the Al-Rawdhatain field show a deterioration in the salinity with time where the fresh groundwater body is concentrated in the central part of the field. The salinity increases toward the borders of the fields. The main groundwater chemistry types based on the most dominant cation and anion concentrations are: $NaHCO_3$, $Ca(HCO_3)_2$, Na_2SO_4, $CaSO_4$, $NaCl$ and $CaCl_2$. The two main groundwater genesis types are Na_2SO_4 and $MgCl_2$ which are present in the aquifer and exhibit continental-marine environmental interaction.

The pH ranges from 7.5-8.5. The EC ranges from 375-4879 µScm^{-1}. The Al-Rawdhatain field is characterized by the presence of alkaline earth's exceeding alkalis and strong acids exceeding weak acids. The computed saturation indices indicate that the groundwater is under saturated with respect to gypsum, anhydrite and halite and oversaturated with respect to calcite and dolomite due to dissolution and precipitation processes. The Al-Rawdhatain field was recharged by Mediterranean precipitation and continental water of meteoric origin. The fresh groundwater represents recent meteoric water.

The mean value of Pco$_2$ is 1.03×10^{-3} atm indicating that the groundwater was charged with CO_2 during infiltration. The geochemical mass balance model shows that mostly calcite is precipitating; dolomite and gypsum are dissolving in all samples. The HCO_3^-/SiO_2 ratio is above 10 and the $SiO_2 < [(Na^+ + K^+) - Cl^-]$ ratio is below 1, indicating that carbonate weathering and the cation exchange are the major chemical reaction processes controlling the chemistry of the groundwater.

The Al-Rawdhatain field represents the only major fresh groundwater resource in Kuwait which is limited with respect to the quantity to a negligible amount of natural recharge. Therefore, the rate of production from the field should be minimized during the Summer months and stopped during the winter months. In addition, to improve the quality of the produced water, the production should occur in the central wells of the aquifer where the salinity is <1000 mgL^{-1}.

ACKNOWLEDGMENT

REFERENCES

AL-RUWAIH, F.M., J.M. Al-Hmoud and Z.M. Al-Dhaferri, 2012. Characterization and evaluation of the confined limestone aquifer in Kuwait. J. Gulf Arabian Peninsula Stud., 3: 17-49.

Al Sharhan, A.S. and A.E.M. Nairn, 1997. Sedimentary Basins and Petroleum Geology of the Middle East. Elsevier, Amsterdam, Netherlands, ISBN: 9781281311603, Pages: 843.

Al-Ruwaih, F., 2001. Hydrochemical investigation on the clastic and carbonate aquifers of Kuwait. Bull. Eng. Geol. Environ., 60: 301-314.

Al-Ruwaih, F.M., L. Talebi and K.M. Hadi, 2005. Major geochemical processes in the evolution of Eocene carbonate aquifer, Kuwait. J. Sci. Eng., 32: 119-144.

Al-Sulaimi, J.S. and F.M. Al-Ruwaih, 2004. Geological, structural and geochemical aspects of the main aquifer systems in Kuwait. Kuwait J. Sci. Eng., 31: 149-174.

Al-Sulaimi, J.S. and F.M. Al-Ruwaih, 2005. Geology and Natural Resources of Kuwait. Academic Publication Council, Kuwait,.

Alhumoud, J.M. and F.M. Al-Ruwaih, 2015. Evaluation and forecasting groundwater consumption in Kuwait. Int. J. Water, 9: 105-120.

Alhumoud, J.M., 2008. Freshwater consumption in Kuwait: Analysis and forecasting. J. Water Supply Res. Technol.-AQUA., 57: 279-288.

Alhumoud, J.M., F.M. Al-Ruwaih and Z.M. Al-Dhafeeri, 2010. Groundwater quality analysis of limestone aquifer of Al-Sulaibiya field, Kuwait. Desalination, 254: 58-67.

Appelo, C.A.J. and D. Postma, 1994. Geochemistry, Groundwater and Pollution. AA Balkema Publisher, Netherlands, pp: 311-313.

Ball, J.W. and D.K. Nordstrom, 1992. Geochemical model to calculate speciation of major, trace and redox elements in natural waters. US. Geological Survey, International Groundwater Modeling Center, USA.

Durov, S.A., 1984. Classification of natural water and graphic representation of composition. Doklady Akad Nauk USSR., 59: 87-90.

Fetter, C.W., 1994. Applied Hydrogeology. 3rd Edn., Prentice-Hall, New Jersey.

Hadi, K.M. and F.M. Al-Ruwaih, 2005. Impact of the environmental deposition on water quality of the limestone aquifer, Kuwait Emirat. J. Eng. Res., 10: 37-49.

Hadi, K.M. and F.M. Al-Ruwaih, 2008. Geochemical evolution of the fresh groundwater in Kuwait desert. Emirates J. Eng. Res., 13: 37-45.

Hounslow, A.W., 1995. Water Quality Data Analysis and Interpretation. Lewis Publishers, New York, USA.,.

Hunt, D.T.E. and A.L. Wilson, 1986. The Chemical Analysis of Water-General Principles and Techniques. 2nd Edn., Royal Society of Chemistry, Burlington House, London. Pages: 683..

Kalhor, K., R. Ghasemizadeh, L. Rajic and A. Alshawabkeh, 2018. Assessment of groundwater quality and remediation in Karst aquifers: A review. Groundwater Sustainable Dev., 8: 104-121.

Marandi, A. and P. Shand, 2018. Groundwater chemistry and the Gibbs Diagram. Applied Geochemistry, 97: 209-212.

Mukhopadhyay, A., J. Al Sulaimi and J.M. Barrat, 1994. Numerical modeling of ground water resource management options in Kuwait. Groundwater, 32: 917-928.

Omar, S.A., A. Al-Yacoubi and Y. Senay, 1981. Geology and groundwater hydrology of the State of Kuwait. J. Arabian Gulf Peninsula Stud., 1: 5-67.

Parkhurst, D.L. and L.N. Plummer, 1993. Geochemical Models in Regional Groundwater Quality. Van Nostrand Reinhold, New York, USA., pp: 199-225.

Plummer, L.N., E.C. Prestemon and D.L. Parkhurst, 1994. An Interactive Code (NETPATH) for Modeling Net Geochemical Reactions along a Flow Path, Version 2.0. Vol. 94, US Geological Survey, Virginia, USA.,.

Salman, S.A., M. Arauzo and A.A. Elnazer, 2019. Groundwater quality and vulnerability assessment in west Luxor Governorate, Egypt. Groundwater Sustainable Dev., 8: 271-280.

Stigter, T.Y., S.P.J. van Ooijen, V.E.A. Post, C.A.J. Appelo and A.M.M. Carvalho Dill, 1998. A hydrogeological and hydrochemical explanation of the groundwater composition under irrigated land in a Mediterranean environment, Algarve, Portugal. J. Hydrol., 208: 262-279.

Sulin, V.A., 1948. Water of Petroleum Formation in System of Natural Waters. USSR, Costoptekhizdat, Moscow,.

Talebi, L.A., 2003. Hydrochemical study and Geological control on groundwater quality of the Dammam Limestone aquifer, Kuwait. MS. Thesis, Kuwait University, Kuwait.

Tleel, J.W., 1973. Surface geology of Dammam dome, Eastern Province, Saudi Arabia. AAPG. Bull., 57: 558-576.

Vanloon, J.C. and R.R. Barefoot, 1989. Analytical Methods for Geochemical Exploration. Academic Press Inc, New York, USA.,.

Wunsch, A., T. Liesch and S. Broda, 2018. Forecasting groundwater levels using nonlinear autoregressive networks with exogenous input (NARX). J. Hydrology, 567: 743-758.